4ICEGE Thessaloniki-GREECE 2007

4th International Conference on
Earthquake Geotechnical Engineering
June 25-28, 2007
Paper No. 1714

THE CHARACTERIZATION OF THE DYNAMIC SOIL PROPERTIES BY MEANS OF A MONTE CARLO INVERSION OF THE RAYLEIGH WAVE DISPERSION CURVE

M. Schevenels, G. Lombaert, G. Degrande, S. François

ABSTRACT

The Spectral Analysis of Surface Waves (SASW) method is a common technique for the identification of the dynamic soil properties. This method consists of an in situ experiment to determine the dispersion curve of the soil and the solution of an inverse problem where the corresponding soil profile is identified. The information on the dynamic soil properties provided by the dispersion curve is limited, however. As a result, the solution of the inverse problem is non-unique. In the present study, a Bayesian approach is followed to solve the inverse problem. The goal of this approach is to obtain a stochastic soil model, accounting for the uncertainty related to the SASW results, that can be used to estimate the transfer functions of the soil. A prior stochastic soil model is first formulated using the information that is available before the SASW test is performed. This prior model is then transformed into a posterior stochastic soil model that accounts for the SASW test results. The posterior model is finally used to predict the response of the soil due to a hammer impact on a foundation. The results are compared with experimental data.

Keywords: dynamic soil characteristics, Spectral Analysis of Surface Waves, stochastic inverse problem, Markov chain Monte Carlo.

INTRODUCTION

The SASW method is a non-invasive method to determine the dynamic shear modulus of shallow soil layers upto a depth of 5 to 10 m (Nazarian & Desai, 1993; Yuan & Nazarian, 1993). The resulting soil profile can be used to solve forced vibrations problems dominated by the wave propagation in the soil, such as the prediction of traffic induced vibrations in the free field or the built environment. The method is based on the dispersive characteristics of surface waves in a layered medium and consists of three steps. The first step involves an in situ experiment where vibrations are generated at the soil's surface using a falling weight, an instrumented impact hammer, or a hydraulic shaker. The free field response is measured with geophones or accelerometers upto a distance of typically 50 m. In the second step, an experimental dispersion curve is determined using the phase of the transfer functions between the receiver signals. It is assumed that the response at sufficiently large distance from the source is dominated by dispersive surface waves. In the third step, an inverse problem is solved to obtain the shear modulus of the soil. The direct stiffness method or the thin layer method (Kausel & Roësset, 1981) is used to calculate the theoretical dispersion curve of a soil with a given shear modulus. The shear modulus is iteratively modified in order to minimize a misfit function defined as the distance between the theoretical and the experimental dispersion curve.

The information on the soil properties provided by the dispersion curve is limited. As a result, the solution of the inverse problem is non-unique: the soil profile obtained with a classical deterministic

Structural Mechanics, K.U.Leuven, Belgium, Email: mattias.schevenels@bwk.kuleuven.be

optimization scheme is only one of the profiles that fit the experimental data. Therefore, alternative solution methods have been developed to identify the ensemble of soil profiles fitting the experimental data (Sambridge & Mosegaard, 2002).

The most robust method to assess the uncertainty on the soil profile is a Monte Carlo simulation where an ensemble of acceptable soil profiles is generated. Monte Carlo inversion techniques usually follow a Bayesian approach (Bayes, 1763). This approach combines the information available before the experiment (the prior information) with the information provided by the experimental data. The prior information is first used to assign a prior probability to every conceivable soil profile. A likelihood function is subsequently defined that reflects the degree to which a given profile fits the experimental data. Finally, the posterior probability of each soil profile is calculated as the (normalized) product of the prior probability and the likelihood. The prior and the posterior probability should be interpreted as the degree of belief that a soil profile is the true soil profile.

Mosegaard & Tarantola (1995) use a Markov chain Monte Carlo inversion technique for a geophysical problem where the density of the soil is derived from the gravity at the soil's surface. The soil is modelled as a layered medium. A prior probability density function (PDF) is formulated for the layer thickness and for the density of each layer. This prior stochastic soil model is sampled by means of a random walk. For each sample, the gravity at the soil's surface is calculated. Next, the Metropolis rule (Hastings, 1970) is used to accept or to reject the sample, depending on the correspondence with the experimental data. In this way, the random walk is modified so that the posterior probability distribution is sampled. The resulting samples represent the ensemble of acceptable soil profiles.

In the present paper, a site in Lincent (Belgium) is considered. An in situ experiment is conducted to determine the experimental dispersion curve of the soil at this site. A Markov chain Monte Carlo method is applied for the inversion of the Rayleigh wave dispersion curve. The final objective is to quantify the uncertainty on the results of a forced vibration problem that depends on the dynamic soil properties. As an example, the uncertainty on the free field field response due to a hammer impact on a concrete foundation is predicted. More complicated problems, such as traffic induced vibrations in the built environment, can be addressed in a similar way. This paper focuses on the identification of the dynamic shear modulus of the soil, although the same methodology can be used to identify the material damping ratio.

THE PRIOR MODEL

In the present paper, the objective of the SASW test is to formulate a soil model for the prediction of the ground vibrations at a site in Lincent (Belgium) due to a hammer impact on a concrete foundation. This vibration prediction problem is addressed in one of the following sections. A preliminary study of this problem shows that the variations of the dynamic shear modulus below a depth of 6 m do not affect the results. It is therefore unnecessary to identify the variations of the shear modulus below 6 m or to include them in the prior stochastic soil model. Hence, the soil is modelled as a homogeneous halfspace overlain by a layer with a thickness $L = 6\,\mathrm{m}$ where the shear modulus varies with depth.

In the layer $0 \leq z \leq L$, the shear modulus is modelled as a random process $\mu(z,\theta)$, where z is the vertical coordinate and θ is the coordinate in the random dimension (Kolmogorov, 1956). In the halfspace $z \geq L$, the shear modulus equals $\mu(L,\theta)$. The other dynamic soil properties are deterministic and constant in both the layer and the halfspace: the Poisson's ratio is $\nu = 1/3$, the density is $\rho = 1800\,\mathrm{kg/m^3}$, and the hysteretic material damping ratio is $\beta = 0.03$ for both dilatational and shear waves. The soil is modelled by means of the direct stiffness method (Kausel & Roësset, 1981), using 60 layer elements with a thickness $d = 0.1\,\mathrm{m}$ on top of a halfspace element.

The shear modulus $\mu(z,\theta)$ is modelled as a stationary non-Gaussian process characterized by a marginal

PDF $p_\mu(\mu)$ and a covariance function $C_\mu(z_1,z_2)$. A lognormal PDF $p_\mu(\mu)$ with mean $m_\mu = 72\,\text{MPa}$ and coefficient of variation $\sigma_\mu/m_\mu = 1$ is used (figure 1a). The choice for a lognormal PDF follows from the prior knowledge that the shear modulus must be positive. The mean value m_μ corresponds to a shear wave velocity $C_s = 200\,\text{m/s}$, which is typical for shallow soil layers in Belgium. The high coefficient of variation stems from the absence of prior information on the variability of the soil properties.

Since the process $\mu(z,\theta)$ is stationary, the covariance function $C_\mu(z_1,z_2)$ can also be written as $C_\mu(z)$ with $z = |z_2 - z_1|$. This function is given by:

$$C_\mu(z) = \sigma_\mu^2 \frac{\pi z}{2l_c} K_1\left(\frac{\pi z}{2l_c}\right) \tag{1}$$

where K_1 is a first order modified Bessel function of the second kind (Abramowitz & Stegun, 1965) and l_c is the correlation length. The function $C_\mu(z)$ belongs to the Matérn class of spatial covariances (Handcock & Stein, 1993). It can be shown that the realizations of a random process with this covariance function are continuous (Kent, 1989), which is a desirable property for a random process used to model the shear modulus of a soil. The choice of the correlation length l_c based on the prior information is a difficult task. A relatively small value $l_c = 0.25\,\text{m}$ is adopted in the present study. In this way, the prior model contains distinct variations of the shear modulus on a small spatial scale compared to the Rayleigh wavelength in the frequency range of interest. The comparison with the resulting small scale variations in the posterior model allows one to assess the resolution of the SASW test. The covariance function $C_\mu(z)$ is shown in figure 1b.

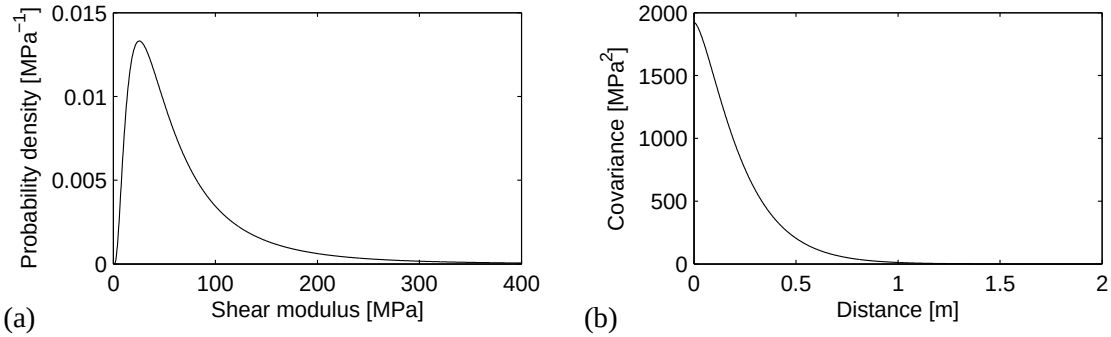

Figure 1: (a) Prior marginal PDF $p_\mu(\mu)$ and (b) prior covariance function $C_\mu(z)$ of the soil's dynamic shear modulus $\mu(z,\theta)$.

In the following, the shear modulus $\mu(z,\theta)$ is discretized so that the random behaviour of the prior model is controlled by a small number of independent Gaussian random variables. Following a method described by Grigoriu (1998), the shear modulus $\mu(z,\theta)$ is modelled as a translation process:

$$\mu(z,\theta) = g\big(\eta(z,\theta)\big) = F_\mu^{-1}\Big(F_\eta\big(\eta(z,\theta)\big)\Big) \tag{2}$$

Herein, $\eta(z,\theta)$ is a standard Gaussian process and g is a memoryless transformation defined in terms of the cumulative density function $F_\mu(\mu)$ of the non-Gaussian process $\mu(z,\theta)$ and the standard Gaussian cumulative density function $F_\eta(\eta)$. The covariance function $C_\eta(z_1,z_2)$ of the underlying Gaussian process $\eta(z,\theta)$ is determined so that the transformation g leads to a non-Gaussian process $\mu(z,\theta)$ with the target covariance function $C_\mu(z_1,z_2)$.

The underlying Gaussian process $\eta(z,\theta)$ is discretized by means of its Karhunen-Loeve decomposition (Ghanem & Spanos, 1991):

$$\eta(z,\theta) \approx \sum_{k=1}^{M} \sqrt{\lambda_k}\, f_k(z)\, \xi_k(\theta) \tag{3}$$

where M is the order of the Karhunen-Loeve decomposition, $\xi_k(\theta)$ are M mutually independent standard Gaussian random variables, and λ_k and $f_k(z)$ are the M highest eigenvalues and corresponding eigenfunctions satisfying the following equation:

$$\int_0^L C_\eta(z_1,z_2)\,f(z_2)\,dz_2 = \lambda\,f(z_1) \tag{4}$$

This integral equation is a homogeneous Fredholm equation of the second kind and can only be solved analytically in very specific cases. It is solved here by means of a Galerkin type procedure developed by Ghanem & Spanos (Ghanem & Spanos, 1991), which is equivalent to the Rayleigh-Ritz method (Baker, 1977). The integral equation (4) has an infinite number of solutions, which are sorted in descending order of eigenvalue λ_k. Only the M lowest order Karhunen-Loeve modes $f_k(x)$, corresponding to the highest eigenvalues λ_k, are withheld in the decomposition (3).

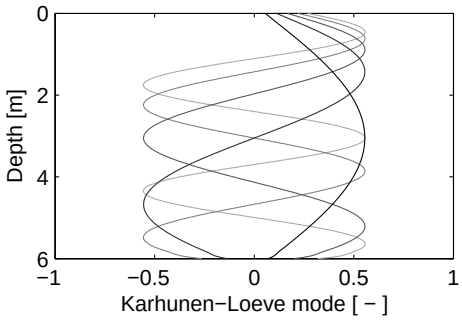

Figure 2: The first five Karhunen-Loeve modes $f_k(z)$ of the underlying Gaussian process $\eta(z,\theta)$. Darker lines represent lower modes.

The first five Karhunen-Loeve modes $f_k(z)$ are shown in figure 2. This figure clearly shows that lower modes vary on a larger scale than higher modes. The number M of modes in the discretization (3) therefore determines the smallest scale on which the variations of the random process $\mu(z,\theta)$ are accounted for. In the present analysis, $M = 16$ Karhunen-Loeve modes are withheld. This choice is based on the convergence of the forced vibration problem in the next section. In the frequency range of interest, the waves that dominate the forced vibration problem do not resolve the higher Karhunen-Loeve modes (Schevenels, et al., 2007). It is therefore unnecessary to identify the contributions of these modes to the random process $\mu(z,\theta)$ or to include them in the prior model.

In order to simulate the random process $\mu(z,\theta)$, a random number generator is used to produce realizations of the random variables $\xi_k(\theta)$. These are introduced in equation (3) to obtain realizations of the underlying Gaussian process $\eta(z,\theta)$, which are finally transformed by means of equation (2) into the realizations of the dynamic shear modulus $\mu(z,\theta)$ shown in figure 3.

THE LIKELIHOOD FUNCTION

For every soil profile, the misfit between the theoretical dispersion curve $C_R^T(\omega)$ and the experimental dispersion curve $C_R^E(\omega)$ is characterized by the likelihood function $L_\xi(\boldsymbol{\xi})$. Herein, $\boldsymbol{\xi}(\theta)$ is a vector collecting the random variables $\xi_k(\theta)$.

The experimental dispersion curve of the soil at the site in Lincent (Belgium) is derived from the phase of the transfer functions between ten pairs of receivers, following Nazarian's method (Nazarian & Desai, 1993). Figure 4 shows the contributions of all pairs to the experimental dispersion curve, as well as an approximating fifth order polynomial. In the following, the polynomial approximation is referred to as the experimental dispersion curve $C_R^E(\omega)$ and used for comparison with the theoretical dispersion curve.

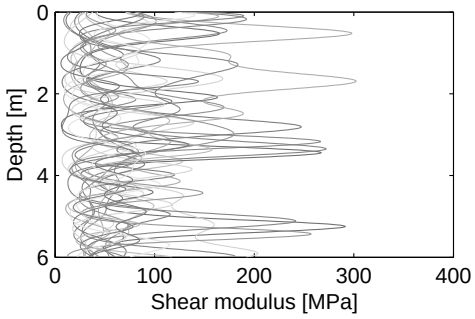

Figure 3: Twenty realizations of the shear modulus $\mu(z,\theta)$ drawn from the prior stochastic soil model.

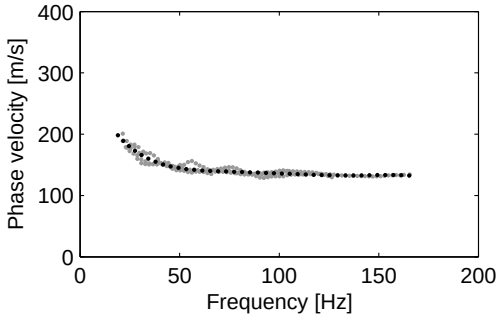

Figure 4: Experimental dispersion curve (gray dots) and approximating polynomial (black dots).

The theoretical dispersion curve is usually calculated as the fundamental solution of a transcendental eigenvalue problem formulated using the direct stiffness method (Kausel & Roësset, 1981) or an equivalent approach. This methodology can lead to erroneous results if the soil contains soft layers overlain by stiffer layers. In such cases, higher-mode Rayleigh waves may affect the surface displacements and the dispersion curve derived from the experimental data may differ from the fundamental Rayleigh wave dispersion curve (Gucunski & Woods, 1991; Tokimatsu, et al., 1992). Several authors have attempted to tackle this problem (Gabriels, et al., 1987; Gucunski & Woods, 1992; Beaty, et al., 2002; Ganji, et al., 1998; Levshin, et al., 2005). In the present study, a methodology similar to the approach of Zomorodian & Hunaidi (2006) is followed. An effective theoretical dispersion curve, accounting for the dominance of higher modes, is calculated as $C_R^T(\omega) = \omega / k_R^T(\omega)$. Here, $k_R^T(\omega)$ is the horizontal wavenumber where the modulus of the Green's function $\tilde{u}_{zz}^G(k_r,\omega)$ at the frequency ω reaches its absolute maximum. The Green's function $\tilde{u}_{zz}^G(k_r,\omega)$ represents the vertical displacements due to a vertical harmonic point load at the soil's surface and is calculated in the frequency-wavenumber domain by means of the direct stiffness method.

The likelihood function $L_\xi(\boldsymbol{\xi})$ is defined as follows in the present study:

$$L_\xi(\boldsymbol{\xi}) = \begin{cases} 0 & \text{if } \max\limits_{\omega} \left| C_R^T(\omega) - C_R^E(\omega) \right| > \Delta C_R \\ 1 & \text{if } \max\limits_{\omega} \left| C_R^T(\omega) - C_R^E(\omega) \right| \leq \Delta C_R \end{cases} \tag{5}$$

where $\Delta C_R = 5\,\mathrm{m/s}$. Hence, all soil profiles for which the deviation of the theoretical dispersion curve $C_R^T(\omega)$ from the experimental dispersion curve $C_R^E(\omega)$ does not exceed the threshold value ΔC_R are acceptable and equally likely, while the other profiles are not acceptable. The choice for this likelihood function is rather arbitrary and subjective. Alternatively, a likelihood function can be formulated on the basis of a more rigorous estimation of the variability of the experimental dispersion curve. O'Neill &

Matsuoka (2005) presents a numerical study of the influence of various sources of uncertainty on the experimental dispersion curve, such as the position and tilt of the sensors. Marosi & Hiltunen (2004) determine the variance of the experimental dispersion curve using a large sample of experimental data collected from two test sites and find a coefficient of variation of 2%. Lai, et al. (2005) follow a similar approach and find coefficients of variation ranging from 1.1% to 5% in the low frequency range and from 0.23% to 1.25% in the high frequency range.

THE BAYESIAN UPDATING SCHEME

In this section, the likelihood function $L_\xi(\boldsymbol{\xi})$ is used to transform the prior soil model into a posterior soil model. The soil models are characterized by a prior PDF $\rho_\xi(\boldsymbol{\xi})$ and a posterior PDF $\sigma_\xi(\boldsymbol{\xi})$, defined in terms of the random variables $\xi_k(\theta)$. In the prior model, these variables are mutually independent and standard Gaussian. Hence, the prior PDF $\rho_\xi(\boldsymbol{\xi})$ is given by:

$$\rho_\xi(\boldsymbol{\xi}) = \frac{1}{(2\pi)^{M/2}} \exp\left(-\frac{\|\boldsymbol{\xi}\|^2}{2}\right) \tag{6}$$

where $\|\boldsymbol{\xi}\|$ is the L_2-norm of the vector $\boldsymbol{\xi}$. Following a Bayesian approach, the posterior PDF is formally defined as:

$$\sigma_\xi(\boldsymbol{\xi}) = k\rho_\xi(\boldsymbol{\xi})L_\xi(\boldsymbol{\xi}) \tag{7}$$

where the normalization constant k is introduced to ensure that the posterior PDF $\sigma_\xi(\boldsymbol{\xi})$ integrates to one. Equation (7) can not be used to obtain a closed-form expression for the posterior PDF $\sigma_\xi(\boldsymbol{\xi})$ since such an expression is not available for the likelihood $L_\xi(\boldsymbol{\xi})$. Therefore, the posterior PDF $\sigma_\xi(\boldsymbol{\xi})$ is not calculated. Instead, a Markov chain Monte Carlo method is applied to obtain a population of soil profiles distributed according to the posterior PDF $\sigma_\xi(\boldsymbol{\xi})$.

The Markov chain is constructed by means of the Metropolis-Hastings algorithm (Hastings, 1970). First, a candidate $\boldsymbol{\xi}'_{i+1}$ for the next state $\boldsymbol{\xi}_{i+1}$ is randomly generated using a conditional PDF $q(\boldsymbol{\xi}'_{i+1}|\boldsymbol{\xi}_i)$ that depends on the current state $\boldsymbol{\xi}_i$ and is referred to as the proposal distribution. Next, the Metropolis-Hastings acceptance probability $r(\boldsymbol{\xi}_i, \boldsymbol{\xi}'_{i+1})$ is calculated as:

$$r(\boldsymbol{\xi}_i, \boldsymbol{\xi}'_{i+1}) = \min\left\{\frac{\sigma_\xi(\boldsymbol{\xi}'_{i+1})}{\sigma_\xi(\boldsymbol{\xi}_i)}\frac{q(\boldsymbol{\xi}_i|\boldsymbol{\xi}'_{i+1})}{q(\boldsymbol{\xi}'_{i+1}|\boldsymbol{\xi}_i)}, 1\right\} \tag{8}$$

Finally, the candidate $\boldsymbol{\xi}'_{i+1}$ for the next state $\boldsymbol{\xi}_{i+1}$ is accepted with probability $r(\boldsymbol{\xi}_i, \boldsymbol{\xi}'_{i+1})$, using an auxiliary random variable with a uniform probability distribution between 0 and 1. If the candidate is rejected then the next state $\boldsymbol{\xi}_{i+1}$ is set equal to the current state $\boldsymbol{\xi}_i$.

Following the approach proposed by Mosegaard & Tarantola (1995), the acceptance or rejection of the candidate state is dealt with in two stages. A candidate state must be accepted in both stages to be admitted to the Markov chain. In the first stage, the acceptance probability $r_1(\boldsymbol{\xi}_i, \boldsymbol{\xi}'_{i+1})$ is calculated from the prior PDF $\rho_\xi(\boldsymbol{\xi})$ as:

$$r_1(\boldsymbol{\xi}_i, \boldsymbol{\xi}'_{i+1}) = \min\left\{\frac{\rho_\xi(\boldsymbol{\xi}'_{i+1})}{\rho_\xi(\boldsymbol{\xi}_i)}\frac{q(\boldsymbol{\xi}_i|\boldsymbol{\xi}'_{i+1})}{q(\boldsymbol{\xi}'_{i+1}|\boldsymbol{\xi}_i)}, 1\right\} \tag{9}$$

The likelihood function $L_\xi(\boldsymbol{\xi})$ is accounted for in the second stage, using the acceptance probability $r_2(\boldsymbol{\xi}_i, \boldsymbol{\xi}'_{i+1})$:

$$r_2(\boldsymbol{\xi}_i, \boldsymbol{\xi}'_{i+1}) = \min\left\{\frac{L_\xi(\boldsymbol{\xi}'_{i+1})}{L_\xi(\boldsymbol{\xi}_i)}, 1\right\} \tag{10}$$

This two-stage approach is equivalent to the use of the acceptance probability $r(\boldsymbol{\xi}_i, \boldsymbol{\xi}'_{i+1})$ defined in equation (8), but the numerical cost is smaller: the likelihood $L_\xi(\boldsymbol{\xi}'_{i+1})$ does not have to be calculated for candidate states that have already been rejected in the first stage.

In the present analysis, the Markov chain is started at a state $\boldsymbol{\xi}_1$ for which the likelihood $L_\xi(\boldsymbol{\xi}_1) = 1$ and stopped after $N = 10^6$ steps. The proposal density $q(\boldsymbol{\xi}'_{i+1}|\boldsymbol{\xi}_i)$ is defined as a Gaussian PDF centered around the current state $\boldsymbol{\xi}_i$:

$$q(\boldsymbol{\xi}'_{i+1}|\boldsymbol{\xi}_i) = \frac{1}{(2\pi)^{M/2}\sigma_q^M} \exp\left(-\frac{\left\|\boldsymbol{\xi}'_{i+1} - \boldsymbol{\xi}_i\right\|^2}{2\sigma_q^{2M}}\right) \tag{11}$$

The standard deviation σ_q determines the step size of the random walk. A larger step size results in a faster exploration of the support of the posterior PDF $\sigma_\xi(\boldsymbol{\xi})$, but also in a lower acceptance rate of candidate states. A standard deviation $\sigma_q = 0.08$ is used, resulting in an acceptance rate of about 0.2.

The proposal density $q(\boldsymbol{\xi}'_{i+1}|\boldsymbol{\xi}_i)$ defined in equation (11) assigns a positive probability to any subset of the vector space of random variables $\xi_k(\theta)$. Hence, the random walk can proceed in a single step from the current state $\boldsymbol{\xi}_i$ to any other state. As a result, the Markov chain is irreducable, aperiodic, and Harris recurrent and can be proven to converge to the posterior PDF $\sigma_\xi(\boldsymbol{\xi})$ for every initial state $\boldsymbol{\xi}_1$ (Tierney, 1994; Robert & Casella, 2004). The convergence of the chain after an infinite number of steps is therefore guaranteed, but it is very difficult to assess the convergence of a chain truncated after a finite number of steps. Robert & Casella (2004) suggest to monitor the convergence of averages and the convergence to independent sampling.

The empirical average $m_{\xi_k}(n)$ and standard deviation $\sigma_{\xi_k}(n)$ of the random variables ξ_k in the Markov chain are calculated as follows:

$$m_{\xi_k}(n) = \frac{1}{n}\sum_{i=1}^{n} \xi_{ik} \tag{12}$$

$$\sigma_{\xi_k}(n) = \sqrt{\frac{1}{n}\sum_{i=1}^{n} \xi_{ik}^2 - m_{\xi_k}^2(n)} \tag{13}$$

The results are shown in figure 5. Both statistics $m_{\xi_k}(n)$ and $\sigma_{\xi_k}(n)$ remain approximately constant after 2×10^5 samples, indicating that the truncated Markov chain has converged.

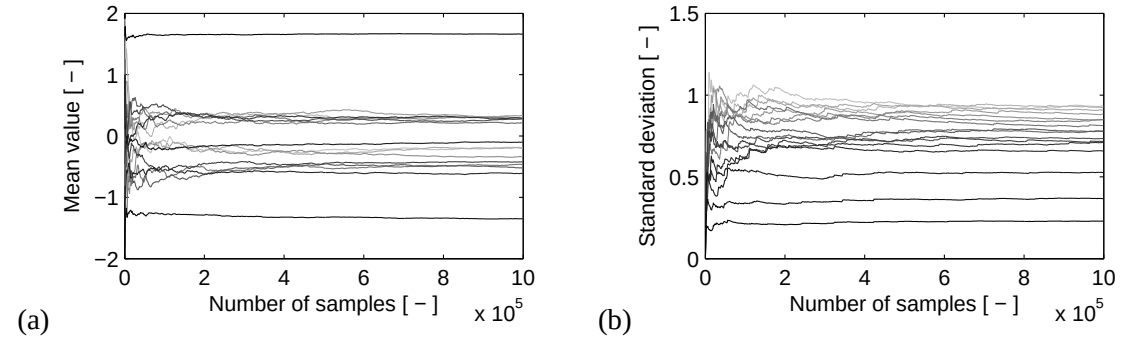

(a) (b)

Figure 5: (a) Mean and (b) standard deviation of the random variables $\xi_k(\theta)$ in the Markov chain. Darker lines correspond to lower Karhunen-Loeve modes.

The convergence to independent sampling is assessed via the correlation coefficients $c_{\xi_k}(\Delta i)$ of subsequent states in the Markov chain. The correlation coefficients $c_{\xi_k}(\Delta i)$ are calculated as follows:

$$c_{\xi_k}(\Delta i) = \frac{1}{\sigma_{\xi_k}^2(N)}\left(\frac{1}{N-\Delta i}\sum_{i=1}^{N-\Delta i} \xi_{ik}\xi_{(i+\Delta i)k} - m_{\xi_k}^2(N)\right) \tag{14}$$

The results are shown in figure 6. The correlation between samples vanishes after about 3000 steps, suggesting that two samples in the Markov chain are mutually independent if they are 3000 or more steps apart from one another. Hence, the chain contains about $10^6/3000 = 333$ mutually independent samples.

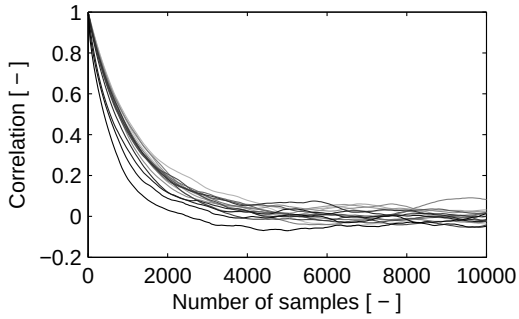

Figure 6: Correlation coefficient $r_{\xi_k}(\Delta i)$ of the random variables $\xi_k(\theta)$ in the Markov chain. Darker lines correspond to lower Karhunen-Loeve modes.

THE POSTERIOR MODEL

The Markov chain constructed in the previous section represents the posterior stochastic soil model. The study of the posterior model and the comparison with the prior model allows us to estimate the resolution of the SASW test. In this section, the resolution of the SASW test is assessed in terms of depth and spatial scale.

Figure 7a shows twenty realizations of the shear modulus $\mu(z,\theta)$ selected from the Markov chain. The corresponding theoretical dispersion curves $C_R^T(\omega)$ are shown in figure 7b and compared with the experimental dispersion curve $C_R^E(\omega)$. The difference between the theoretical and the experimental curves does not exceed the threshold value ΔC_R that has been imposed via the likelihood function $L_\xi(\boldsymbol{\xi})$. Hence, all soil profiles in figure 7a fit the experimental data relatively well. The variability of these profiles is large, however, especially below a depth of 2 m. Below this depth, which equals about 0.2 times the largest wavelength in the experimental dispersion curve, the resolution of the SASW test quickly degrades. A similar observation is made by Beaty et al. (2002).

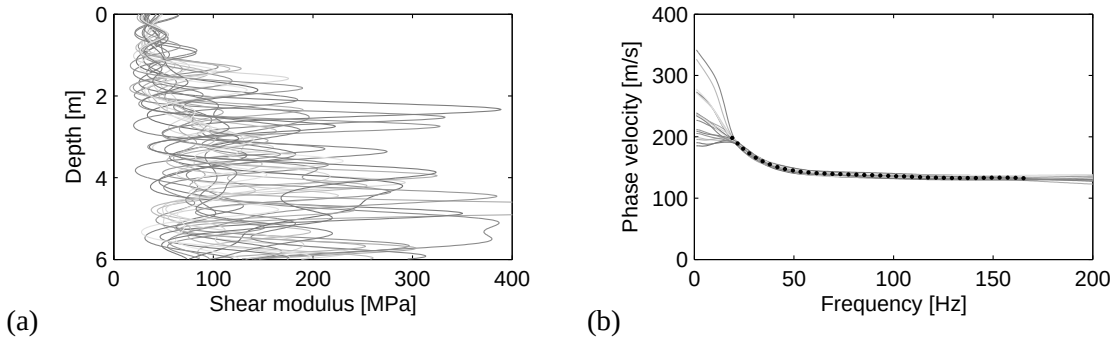

Figure 7: (a) Twenty realizations of the shear modulus $\mu(z,\theta)$ drawn from the posterior stochastic soil model and (b) corresponding theoretical dispersion curves $C_R^T(\omega)$ (gray lines) compared with the experimental dispersion curve $C_R^E(\omega)$ (black dots).

The realizations of the posterior shear modulus $\mu(z,\theta)$ shown in figure 7a exhibit pronounced variations on a small spatial scale compared to the Rayleigh wavelength in the frequency range of interest. These variations contribute substantially to the uncertainty in the posterior soil model, while they depend to a large extent on the small scale variations incorporated in the prior soil model. It is therefore informative to compare the prior and the posterior variability of the shear modulus $\mu(z,\theta)$ on different spatial scales. This is possible via the random variables $\xi_k(\theta)$. In the prior model, the random variables $\xi_k(\theta)$ are mutually independent Gaussian variables with unit variance. In the posterior model, the variables $\xi_k(\theta)$

are no longer independent or Gaussian, and their variance is given by the asymptotes of the curves in figure 5b. The Bayesian updating scheme leads to a reduction of the variance, especially for the variables $\xi_k(\theta)$ corresponding to the lowest Karhunen-Loeve modes in the decomposition of the random process $\eta(z,\theta)$. These modes represent the large scale variations of the shear modulus $\mu(z,\theta)$. Hence, in a SASW test, large scale variations of the shear modulus $\mu(z,\theta)$ are better resolved than small scale variations.

EXPERIMENTAL VERIFICATION

In this section, the prior and the posterior stochastic model of the soil at the site in Lincent (Belgium) are used in a Monte Carlo simulation to predict the uncertainty on the free field vibrations due to a hammer impact on a small surface foundation. The numerical results are compared with experimental data. The free field response is recorded by means of seismic accelerometers located at distances of 8 m and 32 m from the center of the foundation. The free field mobility $M(\omega)$, defined as the transfer function from the hammer force to the free field velocity, is measured using ten hammer impacts on the foundation. For each impact, the free field velocity is calculated from the recorded acceleration by means of the trapezium rule, where a high-pass filter is applied to avoid drifting of the integrated signal.

For 1000 realizations of the stochastic soil model, the free field mobility $M(\omega)$ is numerically predicted. For each of these realizations, a dynamic foundation-soil interaction problem is solved by means of a method based on the subdomain formulation developed by Aubry & Clouteau (1992). The equilibrium equations of the foundation are formulated using a finite element model of the foundation and a boundary element model of the soil (Bonnet, 1995). The boundary element model is based on the Green's functions of a layered halfspace, so that only the foundation-soil interface has to be discretized. In this way, the number of unknowns in the interaction problem is drastically reduced. The Green's functions are calculated in the frequency-wavenumber domain using the direct stiffness method (Kausel & Roësset, 1981) and transformed to the frequency-spatial domain by means of the inverse Hankel transform algorithm developed by Talman (1978). Finally, the 95% confidence region of the modulus $|M(\omega)|$ of the mobility is estimated from the simulations.

Figures 8 and 9 show twenty realizations and the 95% confidence region of the modulus $|M(\omega)|$ of the free field mobility, calculated with the prior and the posterior stochastic soil model, respectively. The results are compared with the experimental data.

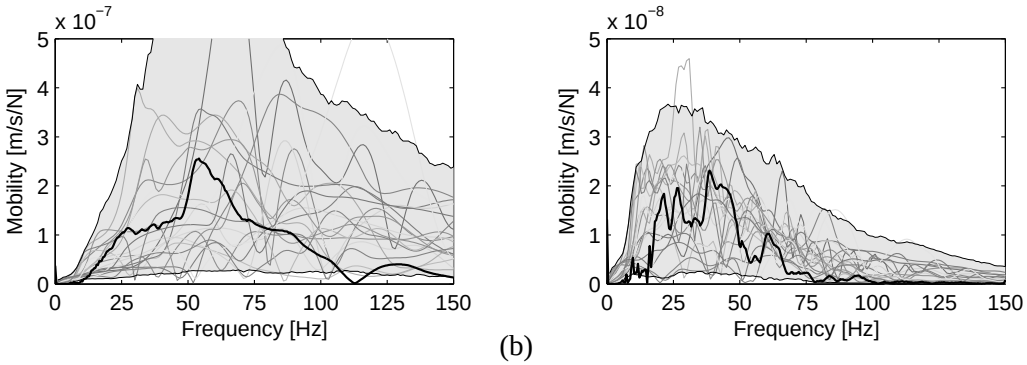

(a) (b)

Figure 8: Twenty realizations (gray lines) and 95% *confidence region (gray area) of the prior free field mobility modulus* $|M(\omega)|$ *compared with the experimental data (black line) for a source-receiver distance of (a)* 8 m *and (b)* 32 m.

Compared to the prior mobility, the variability of the posterior mobility is smaller. The strongest reduction of the variability is observed in the low frequency range (below 40 Hz). In this range, the wavelengths of the dominating waves in the soil are large compared to the scale of the variations of the shear modulus

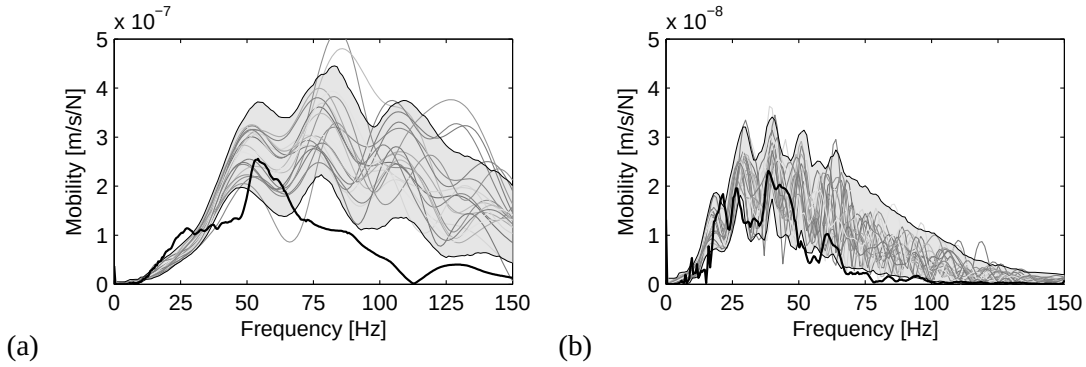

Figure 9: Twenty realizations (gray lines) and 95% *confidence region (gray area) of the posterior free field mobility modulus* $|M(\omega)|$ *compared with the experimental data (black line) for a source-receiver distance of (b)* 8 m *and (b)* 32 m.

$\mu(z,\theta)$ that are not uniquely identified by the SASW method. Hence, the waves do not resolve these small scale variations. Therefore, the mobility $M(\omega)$ is relatively insensitive to the uncertainty on the soil profile derived from the SASW test. All profiles in the posterior stochastic soil model are, to a certain degree, equivalent with respect to the prediction of the mobility. This implies that a single solution of the inverse problem in the SASW method, obtained using a deterministic inversion procedure, can be used for a reliable prediction of the mobility in the low frequency range. This approach can also be followed for the prediction of road traffic induced vibrations in the free field or the built environment, since the dominant frequency of road traffic induced vibrations is about 10 Hz.

In the high frequency range, the reduction of the variability of the posterior mobility is less pronounced. In this range, the wavelengths are smaller and the waves in the soil are affected by the small scale variations of the shear modulus $\mu(z,\theta)$. Hence, the predicted free field mobility is affected by the uncertainty on the SASW results. This implies that the use of a soil profile obtained from a SASW test and a deterministic inversion procedure can lead to an inaccurate prediction of the mobility in the high frequency range. Similar conclusions hold for problems such as the prediction of rail traffic induced vibrations, where the dominant frequency may be above 50 Hz. In such cases, the variability on the soil profile derived from the SASW test should be accounted for, or a different soil investigation technique with a finer resolution should be used.

The correspondence of the measured and the predicted free field mobility in figure 9 is satisfactory in the low frequency range. In the high frequency range, the mobility is overestimated. This discrepancy between measured and predicted results might be caused by a too restrictive prior stochastic soil model, leading to a biased posterior soil model. The prior model only allows the shear modulus to vary, the other material properties are kept constant. The soil is also assumed to be layered so that variations of the shear modulus in the horizontal direction are prohibited. Another explanation of the discrepancy is possibly non-linear behaviour of the soil under the foundation.

CONCLUSION

In the present paper, the determination of the dynamic shear modulus of shallow soil layers from a SASW test is addressed in a probabilistic framework. A Bayesian updating technique is used to identify an ensemble of soil profiles that fit the experimental dispersion curve. First, the prior information on the soil properties is used to construct a prior stochastic soil model. The variations of the shear modulus with depth are modelled by means of a random process, which is discretized by means of the Karhunen-Loeve decomposition of an underlying Gaussian process. Next, a Markov chain Monte Carlo method is applied to sample the prior stochastic soil model. For each sample, the theoretical dispersion curve is

calculated and compared with the experimental dispersion curve. The Metropolis rule is used to accept or reject each sample based on the correspondence of both curves. In this way, only the soil profiles that fit the experimental data are withheld and a population of profiles is obtained that follows the posterior stochastic soil model. The posterior model accounts for both the prior information and the measurement data. The prior and the posterior stochastic soil model are compared to assess the resolution of the SASW method. It is observed that the variations of the shear modulus on a large spatial scale are well resolved, especially in a region near the soil's surface. The resolution deteriorates as the spatial scale decreases and the depth increases. Finally, the posterior stochastic soil model is used in a Monte Carlo simulation to quantify the uncertainty on the results of a vibration prediction problem. The variability of the free field field response due to a hammer impact on a concrete foundation is predicted. An experiment is conducted to verify the results of this simulation. It is shown that the variability is small in the low frequency range and large in the high frequency range. Hence, for vibration predictions in the low frequency range, the classical SASW method where a deterministic inversion procedure is used to identify the soil profile gives reliable results. For vibration predictions in the high frequency range, however, the uncertainty on the soil profile derived from the SASW test has an impact on the response. In such cases, this uncertainty should be accounted for or a different soil investigation method with a finer resolution should be used.

REFERENCES

M. Abramowitz & I. Stegun (1965). *Handbook of mathematical functions*. Dover, New York.

D. Aubry & D. Clouteau (1992). 'A subdomain approach to dynamic soil-structure interaction'. In V. Davidovici & R. Clough (eds.), *Recent advances in Earthquake Engineering and Structural Dynamics*, pp. 251–272. Ouest Editions/AFPS, Nantes.

C. Baker (1977). *The numerical treatment of integral equations*. Clarendon Press, Oxford.

T. Bayes (1763). 'An essay towards solving a problem in the doctrine of chances'. *Philosophical Transactions of the Royal Society* **53**:370–418.

K. Beaty, et al. (2002). 'Simulated annealing inversion of multimode Rayleigh wave dispersion curves for geological structure'. *Geophysical Journal International* **151**:622–631.

M. Bonnet (1995). *Boundary integral equation methods for solids and fluids*. John Wiley and Sons, England.

P. Gabriels, et al. (1987). 'In situ measurements of shear-wave velocity in sediments with higher-mode Rayleigh waves'. *Geophysical Prospecting* **35**:187–196.

V. Ganji, et al. (1998). 'Automated inversion procedure for Spectral Analysis of Surface Waves'. *Journal of Geotechnical and Geoenvironmental Engineering, Proceedings of the ASCE* **124**(8):757–770.

R. Ghanem & P. Spanos (1991). *Stochastic finite elements: a spectral approach*. Springer-Verlag, New York.

M. Grigoriu (1998). 'Simulation of stationary non-Gaussian translation processes'. *Journal of Engineering Mechanics, Proceedings of the ASCE* **124**(2):121–126.

N. Gucunski & R. Woods (1991). 'Inversion of Rayleigh wave dispersion curve for SASW test'. In *Proceedings of the 5th International Conference on Soil Dynamics and Earthquake Engineering*, pp. 127–138, Karlsruhe.

N. Gucunski & R. Woods (1992). 'Numerical simulation of the SASW test'. *Soil Dynamics and Earthquake Engineering* **11**:213–227.

M. Handcock & M. Stein (1993). 'A Bayesian analysis of kriging'. *Technometrics* **35**(4):403–410.

W. Hastings (1970). 'Monte Carlo sampling methods using Markov chains and their applications'. *Biometrika* **57**(1):97–109.

E. Kausel & J. Roësset (1981). 'Stiffness matrices for layered soils'. *Bulletin of the Seismological Society of America* **71**(6):1743–1761.

J. Kent (1989). 'Continuity properties for random fields'. *The Annals of Probability* **17**(4):1432–1440.

A. Kolmogorov (1956). *Foundations of the theory of probability*. Chelsea Publishing Company, New York.

C. Lai, et al. (2005). 'Propagation of data uncertainty in surface wave inversion'. *Journal of Environmental and Engineering Geophysics* **10**(2):219–228.

A. Levshin, et al. (2005). 'The use of crustal higher modes to constrain crustal structure across Central Asia'. *Geophysical Journal International* **160**:961–972.

K. Marosi & D. Hiltunen (2004). 'Characterization of spectral analysis of surface waves shear wave velocity measurement uncertainty'. *Journal of Geotechnical and Geoenvironmental Engineering, Proceedings of the ASCE* **130**(10):1034–1041.

K. Mosegaard & A. Tarantola (1995). 'Monte Carlo sampling of solutions to inverse problems'. *Journal of Geophysical Research* **100**:12431–12447.

S. Nazarian & M. Desai (1993). 'Automated surface wave method: field testing'. *Journal of Geotechnical Engineering, Proceedings of the ASCE* **119**(7):1094–1111.

A. O'Neill & T. Matsuoka (2005). 'Dominant Higher Surface-wave Modes and Possible Inversion Pitfalls'. *Journal of Environmental and Engineering Geophysics* **10**(2):185–201.

C. Robert & G. Casella (2004). *Monte Carlo statistical methods*. Springer, New York.

M. Sambridge & K. Mosegaard (2002). 'Monte Carlo methods in geophysical inverse problems'. *Reviews of Geophysics* **40**(3):1–29.

M. Schevenels, et al. (2007). 'The Green's functions of a vertically inhomogeneous soil with a random dynamic shear modulus'. *Probabilistic Engineering Mechanics* **22**(1):100–111.

J. Talman (1978). 'Numerical Fourier and Bessel transforms in logarithmic variables'. *Journal of Computational Physics* **29**(1):35–48.

L. Tierney (1994). 'Markov chains for exploring posterior distributions'. *The Annals of Statistics* **22**(4):1701–1762.

K. Tokimatsu, et al. (1992). 'Effects of multiple modes on Rayleigh wave dispersion characteristics'. *Journal of Geotechnical Engineering, Proceedings of the ASCE* **118**(10):1529–1143.

D. Yuan & S. Nazarian (1993). 'Automated surface wave method: inversion technique'. *Journal of Geotechnical Engineering, Proceedings of the ASCE* **119**(7):1112–1126.

S. Zomorodian & O. Hunaidi (2006). 'Inversion of SASW dispersion curves based on maximum flexibility coefficients in the wave number domain'. *Soil Dynamics and Earthquake Engineering* **26**:735–752.